



The role of loop and beta-turn residues as structural and functional determinants for the lipoyl domain from the *Escherichia coli* 2-oxoglutarate dehydrogenase complex

D Dafydd Jones, Richard N Perham

► To cite this version:

D Dafydd Jones, Richard N Perham. The role of loop and beta-turn residues as structural and functional determinants for the lipoyl domain from the *Escherichia coli* 2-oxoglutarate dehydrogenase complex. *Biochemical Journal*, 2007, 409 (2), pp.357-366. 10.1042/BJ20071119 . hal-00478872

HAL Id: hal-00478872

<https://hal.science/hal-00478872>

Submitted on 30 Apr 2010

HAL is a multi-disciplinary open access archive for the deposit and dissemination of scientific research documents, whether they are published or not. The documents may come from teaching and research institutions in France or abroad, or from public or private research centers.

L'archive ouverte pluridisciplinaire **HAL**, est destinée au dépôt et à la diffusion de documents scientifiques de niveau recherche, publiés ou non, émanant des établissements d'enseignement et de recherche français ou étrangers, des laboratoires publics ou privés.

Running title: Determinants of E2o lipoyl domain structure and function

The role of loop and β -turn residues as structural and functional determinants for the lipoyl domain from the *Escherichia coli* 2-oxoglutarate dehydrogenase complex.

D. Dafydd Jones*¹ & Richard N. Perham.

Department of Biochemistry, University of Cambridge, 80 Tennis Court Road, Cambridge CB2 1GA, UK.

Present address: D. D. Jones, School of Biosciences, Cardiff University, Museum Avenue, CF10 3US, UK.

¹ Correspondence: D. D. Jones, School of Biosciences, Museum Avenue, Cardiff University, Cardiff CF10 3US, UK. Tel: +44 (0)29 20874290; Email: jonesdd@cf.ac.uk.

Keywords: Lipoyl domain, protein-protein interactions, 2-oxoglutarate dehydrogenase, substrate channelling, post-translational modification, protein misfolding.

Abbreviations: 2OGDH, 2-oxoglutarate dehydrogenase complex; E1, 2-oxo acid decarboxylase; E1o, 2-oxoglutarate decarboxylase; E1p, pyruvate decarboxylase; E2, dihydrolipoyl acyltransferase; E2o, dihydrolipoyl succinyltransferase; E2olip, lipoyl domain from 2OGDH complex; E2plip, lipoyl domain from PDH complex; LplA, lipoate protein ligase A; ND-PAGE, non-denaturing poly acrylamide gel electrophoresis; PDH, pyruvate dehydrogenase.

Abstract

The lipoyl domain of the dihydrolipoyl succinyltransferase (E2o) component of the 2-oxoglutarate dehydrogenase (2OGDH) multi-enzyme complex houses the lipoic acid cofactor through covalent attachment to a specific lysine side-chain residing at the tip of a β -turn. Residues within the lipoyl-lysine β -turn and a nearby prominent loop have been implicated as determinants of lipoyl domain structure and function. Protein engineering of the *E. coli* E2o lipoyl domain (E2olip) revealed that removal of residues from the loop caused a major structural change in the protein, which rendered the domain incapable of reductive succinylation by 2-oxoglutarate decarboxylase (E1o) and reduced the lipoylation efficiency. Insertion of a new loop corresponding to that of the *E. coli* pyruvate dehydrogenase lipoyl domain (E2plip) restored lipoylation efficiency and the capacity undergo reductive succinylation returned, albeit at a lower rate. Exchange of the E2olip loop sequence significantly improved the ability of the domain to be reductively acetylated by pyruvate decarboxylase (E1p), retaining *ca* 10 fold more acetyl group after 25 min than wild-type E2olip. Exchange of the β -turn residue on the N-terminal side of the E2o lipoyl-lysine DK^{A/V} motif to the equivalent residue in E2plip (T42G), both singly and in conjunction with the loop exchange, reduced the domain's ability to be reductively succinylated, but lead to an increased capacity to be reductively acetylated by the non-cognate E1p. The T42G mutation also slightly enhanced the lipoylation rate of the domain. The surface loop is important to the structural integrity of the protein and together with Thr42 plays an important role in specifying the interaction of the lipoyl domain with its partner E1o in the *E. coli* 2OGDH complex.

Introduction

The 2-oxo acid dehydrogenase multienzyme complexes play pivotal roles in metabolism. They catalyse the oxidative decarboxylation of 2-oxo acids, generating NADH and the corresponding acyl coenzyme A. The three main members of the family are pyruvate (PDH), 2-oxoglutarate (2OGDH) and branched-chain 2-oxo acid dehydrogenase complexes, the substrates for the latter being the 2-oxo acids produced by the transamination of valine, leucine and isoleucine [1-3]. The 2OGDH complex catalyses the conversion of 2-oxoglutarate (α -ketoglutarate) to succinyl CoA as part of the Krebs/tricarboxylic acid cycle. The complex is composed of three component enzymes, 2-oxoglutarate decarboxylase (E1o; EC 1.2.4.2), dihydrolipoyl acetyltransferase (E2o; EC 2.3.1.6) and dihydrolipoyl dehydrogenase (E3; EC 1.8.1.4), with the corresponding enzymes found in the PDH and branched chain 2-oxo acid dehydrogenase complexes [2, 4]. E1 catalyses the initial decarboxylation of the 2-oxo acid, using thiamin diphosphate (ThDP) as a cofactor, and then reductively acylates a lipoyl group bound in N^6 -amide linkage to a specific lysine residue in E2 subunit. E2 is an acyltransferase responsible for transferring the acyl group on to CoA, and the dihydrolipoyl group left on E2 is finally reoxidized back to the dithiolane ring configuration by the flavoprotein E3, with NAD^+ as the ultimate electron acceptor. E1 and E2 differ from complex to complex, whereas E3 is generally common to the different complexes in a given organism.

The structural core of the complex is provided by E2, with E1 and E3 bound around the periphery [2, 3, 5, 6]. The E2 chains are highly segmented comprising, from the N-terminus, one to three lipoyl domains (*ca* 9 kDa), a peripheral subunit-binding domain (*ca* 4 kDa), and an acyltransferase domain (*ca* 28 kDa) [2, 4]. The E2o chain of 2OGDH contains a single lipoyl domain and an assembly of 24 separate acyltransferase domains arranged with octahedral symmetry form the core of the complex. The E2p chain of PDH from *Escherichia coli* and other Gram-negative bacteria is similar, except that it contains three lipoyl domains [2, 4]. In all these cases, the domains comprising the E2 chains are separated by long (25-30 residue) segments of polypeptide chain characteristically rich in alanine, proline and charged amino acids, which forms a flexible and extended linker region [2].

The three dimensional structure of various lipoyl domains have been solved in recent years, including those from *E. coli* PDH [7, 8] and 2OGDH [9] (Figure 1), *Azotobacter vinelandii* PDH [10] and 2OGDH [11], and human PDH [12] and branched-chain 2-oxo acid dehydrogenase [13]. The overall fold of all lipoyl domains is identical, comprising a flattened β -barrel formed by two four-stranded β -sheets with a two-fold axis of quasi-symmetry. The symmetrical relationship of the N- and C-terminal halves of lipoyl domains also extends to

the positioning of the hydrophobic core residues [8]. The symmetry of the two halves of the protein is broken by the presence of a prominent surface loop linking strands 1 and 2. The lipoyl-lysine residue is found at the tip of a protruding type I β -turn. The exact positioning of the lysine within the β -turn is essential for attachment of the lipoic acid to the protein by a group of enzymes collectively known as the lipoate protein ligase [14, 15].

One of the key interactions in the complex central to catalysis is that between the E1 component and the lipoyl domain of E2. While free lipoate can act as the substrate for E2 and E3, the lipoylated lipoyl domain is the true substrate for reductive acylation by E1, raising the value of k_{cat}/K_m by a factor of 10^4 compared to free lipoate [16, 17]. Moreover, the lipoyl domains from the PDH and 2OGDH complexes only function as efficient substrates for their respective E1p and E1o components [18-20]. Thus, the lipoyl domain is critical to the activation of the pendant lipoyl moiety for its use as a substrate for E1 and as a determinant of substrate channelling that ensures only a specific lipoyl group attached to the intended E2 component is reductively acylated [2, 21, 22]. The recently solved structures of E1p [23-25] and E1o [26] support the requirement for a specific interaction between the lipoyl domain and E1 as the ThDP is buried within the protein and requires the lipoyl domain to make close contact [27].

How the interaction between E1 and the lipoyl domain activates and specifies the lipoyl group to be reductively acylated is still not fully understood. The binding of the lipoyl domain to *E. coli* E1p is weak (K_s not less than 1 mM despite a K_m of *ca* 20 μ M) and transient [19]. NMR interaction studies with the innermost *E. coli* PDH lipoyl domain (E2plip) indicated that the apo form of the domain does not interact with E1o, but once the domain is lipoylated it does interact with E1o albeit in a non-productive manner [28]. It is thought that the interaction is restricted to the lipoyl moiety, providing further evidence that the lipoyl domain is an essential catalytic requirement and that reductive acylation by E1 is ultimately determined by the lipoyl domain.

Several protein engineering and NMR investigations have suggested that the prominent surface loop that links the first and second β -strands and lies close in space to the lipoyl-lysine β -turn (Figure 1a) is an important determinant of the interaction with E1p in various PDH complexes [18, 20, 29]. The loop also appears to be an important structural determinant for the E2plip domains [20]. The residue immediately adjacent to lipoyl-lysine motif ($\text{DK}^{\text{A}}/\text{V}$) was also thought to be involved in specifying the interaction with E1. Mutation of this residue (referred to from herein as the XDK residue) in *Bacillus stearothermophilus* E2plip (N40A) resulted in a lower rate of reductive acetylation [29, 30]. However, mutation of the

equivalent residue in *E. coli* E2plip (G39T) did not greatly influence reductive acetylation [20].

Here we investigate if the prominent surface loop and residues surrounding the lipoyl-lysine residue play an important role in determining the structural and functional properties of the *E. coli* 2OGDH complex lipoyl domain (E2olip). As with the *E. coli* E2plip domain, we show that the prominent surface loop in E2olip is important for the structural integrity of the domain and plays a key role in defining the interaction with E1o. However, unlike the E2plip domain from *E. coli*, we discovered that the XDK residue immediately N-terminal to the lipoyl-lysine motif also plays a key role in defining the interaction between E2olip and E1o. We also show that by exchanging both loop and XDK residues in E2olip for their equivalents in E2plip, the ability of the domain to undergo a productive interaction with the non-cognate E1p increases significantly. Our observations support the idea that these regions of E2olip are important contributors but not the sole determinants of specificity in reductive acylation and hence substrate channelling through the complex. We also show that the process of lipoylation by lipoate protein ligase A (LplA) is far less sensitive to changes in E2olip structure, and occurs even when there are substantial changes to the conformation of the domain.

Materials and Methods

Materials

Sodium [2-¹⁴C] pyruvate and sodium [5-¹⁴C] 2-oxoglutarate were obtained from NEN Research Products and American Radiolabels Inc., respectively. Oligonucleotides were synthesized by Dr Charles Hill of the Protein and Nucleic Acid Chemistry Facility (PNAC), Department of Biochemistry, University of Cambridge. All DNA modifying enzymes were purchased from NE Biolabs unless otherwise stated. All other chemicals used were of analytical grade. *E. coli* lipoyl protein ligase A (LplA) was kindly prepared by Mr C. Fuller as described elsewhere [31].

Protein engineering of the E2o domain

Modification of the E2olip loop sequence was performed using a cassette mutagenesis strategy, similar to that reported previously for E2plip [20] and described in detail in the Supplementary Information. The T42G and V45A point mutations were introduced using the splice-overlap extension PCR method [32, 33] using the mutagenic oligonucleotides indicated in Supplementary Table 1 in conjunction with primers based on the pET11c DNA sequence flanking the insert. Splice-overlap PCR was performed using *Pfu* DNA polymerase (Stratagene). All mutated genes encoding the variant E2olip domains were cloned between the NdeI and BamHI sites of pET11c for their over-expression in *E. coli*. Unlabelled and ¹⁵N-labelled wild-type and mutant E2olip domains were over-expressed and produced in *E. coli* BL21(DE3) cells and purified (as apo-forms) as described previously [9, 20].

Lipoylation of the *E. coli* lipoyl domains *in vitro*

The apo-forms of the domains were lipoylated *in vitro* by exposure to *E. coli* LplA in the presence of lipoic acid, as described elsewhere [20]. The products were separated by anion exchange chromatography using a Resource-QTM column (Pharmacia) developed with an ammonium bicarbonate gradient, essentially as described previously [20, 34]. The lipoylated domains were buffer-exchanged into 20 mM sodium phosphate, pH 7.0, and their identity, including the correct post-translational modification, was confirmed by means of electrospray mass spectrometry.

To assess the rate of lipoylation, the apo-form of the lipoyl domain (50 µM) was incubated with 1.2 mM ATP, 1.2 mM MgCl₂ and 0.6 mM sodium lipoate in 20 mM Tris-HCl, pH 7.5, for 5 min at 25°C. LplA was added to a concentration of 20 µg/ml. At various times, samples (0.4 nmol) of lipoyl domain were removed, mixed with a 20-fold molar excess of EDTA over MgCl₂ and submitted to either non-denaturing PAGE (ND-PAGE) on a 20% acrylamide gel to separate the apo- and holo-forms of the domain or electrospray mass spectrometry. For analysis by ND-PAGE, samples were taken at 1, 2, 5 10, 30 and 90 min. For analysis by

electrospray mass spectrometry, samples were taken at 5, 15, 35, 45 and 60 min. The samples were buffer exchanged into water using a Millipore Biomax-5 0.5 centrifugal unit before performing mass spectrometry.

Reductive acylation of the lipoyl domains

Reductive acylation of the lipoyl domain in the presence of a given 2-oxo acid was measured using the method reported previously [20] and is described in detail in the Supplementary Information.

NMR spectroscopy

All NMR spectra were obtained with a Bruker AM500 spectrometer at 298K. 2D ^1H NOESY spectra [35, 36] were recorded using water suppression by presaturation and a mixing time of 100 ms, and 32 scans with 2048 data points in the t_2 dimension and 512 increments in t_1 , with a spectral width of 8064.52 Hz. All ^{15}N HSQC spectra were recorded using 16 scans for each t_1 time point and with 300 increments with corresponding acquisition times of 0.127 s for the directly acquired dimension and 0.326 s for the indirectly acquired dimension. The ^1H and ^{15}N spectral widths were 8064.62 Hz and 927.29 Hz, respectively. Samples of lipoyl domain (2-3 mM) were dissolved in 20 mM sodium phosphate buffer, pH 6.0, containing 10% (v/v) D_2O , 0.05% (w/v) sodium azide and 40 μM trimethylsilyl propionate (TSP) as the internal reference for ^1H chemical shift. Data were processed using the Azara suite of programs (W. Boucher, unpublished work). Resonance assignment was performed using the program ANSIG [37]. Resonance assignments of the wild-type E2olip domain had been performed previously [9] and formed the basis for assignment of resonances associated with the mutant domains. To confirm correct assignment of peaks in the spectra of mutant proteins, through bond connectivities were established from TOCSY or HSQC-TOCSY spectra, and through-space connectivities were identified from 2D ^1H NOESY or ^{15}N HMQC-NOESY [8,9] spectra to verify sequential assignments. The chemical shift differences were calculated by subtracting the chemical shifts of wt E2olip from those of the mutant domain. The ^{15}N chemical shift differences were factored down by $1/7$ to normalise them to ^1H values (based on a ^{15}N chemical shift range of *ca* 32 ppm for ^{15}N compared to *ca* 4.5 ppm for ^1H).

General techniques

E. coli E1p and E1o were both the products of genes over-expressed in *E. coli*, and purified as described previously [20, 23, 26]. Protein concentrations of lipoyl domains were determined by amino acid analysis, kindly performed by Mr Peter Skerit of the PNAC facility, University of Cambridge. Samples for positive-ion electrospray mass spectrometry were prepared in aqueous acetonitrile (50% v/v) containing formic acid (1% v/v) and

analysed on a VG BioQ quadrupole mass spectrometer using myoglobin as the standard. ND-PAGE was performed as described previously [20, 31], except that pH values of the resolving and stacking gels were 8.5 and 6.5, respectively. The gels were stained with Coomassie Brilliant Blue. The extent of lipoylation was estimated by densitometric analysis of the bands representing the apo- and holo-forms of the domain, the latter migrating more rapidly towards the anode.

Results

Design of E2olip variants

All known structures of lipoyl domains, including *E. coli* E2olip (Figure 1a) [9] and E2plip [8], have a prominent surface loop linking the first and second β -strands that lies close in space to the exposed β -turn housing the lipoyl-lysine residue. The equivalent region in the C-terminal symmetrical half of lipoyl domains is generally shorter by 4-6 residues (Figure 1b and [20]), depending on the source of the lipoyl domain. The surface loop is thought to be a key determinant in specifying the interactions of the domain with E1 and in maintaining the functional conformation of the protein [18, 20, 28, 29]. Therefore, it was decided to mutate the loop and test the effect on the structure, post-translational modification and reductive acylation of the domain.

The loop length is critical for maintaining the functional conformation of *E. coli* E2plip as deletion of the four residues absent for the equivalent region in the C-terminal half of the protein causes the protein to assume an alternative conformation. To test if the loop plays a similar role in E2olip, the prominent surface loop was also shortened by removal of the PESVAD sequence absent from the equivalent region in the C-terminal half so creating E2olipLD (Figure 1b and c). To test the role of the loop in specifying the interaction of E2olip with E1o, the E2olipLS variant was constructed by replacement of the PESVAD sequence with the equivalent region from the E2plip domain (GGDE; [20]). The loop exchange was also expanded into the N-terminal section of β -strand 2 to create the E2olipLS+ variant by the incorporation of two additional mutations (A17V and T18E; Figure 1c) to investigate if the specificity region extends beyond the loop.

The XDK residue is closely associated with both the lipoyl-lysine and the prominent surface loop (Figure 1a) and is thought to play a major role specifying the interaction with E1p in some E2plip, such as *B. stearotherophilus* PDH [29], but not others including *E. coli* PDH [20]. In the E2olip domain from various species, the XDK residue is generally a threonine (Thr42 in *E. coli* E2olip) but the equivalent residue in *E. coli* E2plip is glycine. Therefore, the T42G mutation was introduced into both the wt E2olip and E2olipLS to investigate the influence of this residue in specifying the interaction of the domain with E1o and E1p. The residue following the lipoyl-lysine also shows variability between E2olip and E2plip. This residue is valine in E2olip from various organisms (Val45 in *E. coli* E2olip) but in E2plip it is usually an alanine. Therefore, the V45A mutation was introduced into *E. coli* E2olip to investigate its role in determining the interaction with E1. All the E2olip variants are summarised in Figure 1c.

***In vitro* lipoylation of the E2olip domains**

All the mutant E2olip proteins were over-expressed in *E. coli* and purified as soluble proteins. Due to the high level production of E2olip and its variants in *E. coli*, all the domains were purified in their unlipoylated form, as shown by electrospray mass spectrometry (Table 1). Unlike E2plip, the N-terminal methionine of wt E2olip and its variants was fully processed (Table 1).

All the domains could be lipoylated *in vitro* using lipoate protein ligase A (LplA), as determined by electrospray mass spectrometry (Table 1). Wild-type E2olip was lipoylated at a similar rate to that of wt E2plip (Figure 2). Observations made by Jones *et al.*, [20] indicated that the presence of E2olip surface loop within E2plip may determine lipoylation efficiency. As both wt E2olip and wt E2plip were lipoylated at similar rates, this would suggest that the loop sequence itself does not act as a determinant of lipoylation efficiency. This is substantiated by the observation that lipoylation of E2olipLS was not hindered but occurred at a similar rate to that of the wt E2olip (Table 1). All the E2olip variants, apart from E2olipLD were fully lipoylated by 60 min, as judged by electrospray mass spectrometry (Table 1). Mass spectrometry analysis of samples taken during the 60 min period suggests that the lipoylation rate was similar for wt E2olip, E2olipLS and E2olipLS+ (Table 1), with just over 50% of the domain being lipoylated within 30 min and greater than 75% of the domain observed to be lipoylated after 45 min (data not shown). Therefore, introducing the smaller loop from E2plip into E2olip had no adverse effect on the capacity of the domain to be lipoylated. For both E2plipT42G and E2plipLS-T42G, full lipoylation was observed within 45 min. While it can be safely inferred that the T42G mutation has not significantly affected the structure of the lipoyl-lysine β -turn, the slightly enhanced lipoylation rate suggests that the domain is more amenable to post-translational modification. The E2olipLD domain was lipoylated at a rate much lower than wild-type E2olip, as observed by both ND-PAGE (Figure 2) and verified by electrospray mass spectrometry (Table 1).

Reductive acylation of the E2olip surface loop variants

The E2olipLS and E2olipLS+ variants with the interchanged surface loop and the E2olipLD loop deletion variant (Figure 1c) were assayed for their ability to become reductively succinylated (by E1o in the presence of 2-oxoglutarate) and acetylated (by E1p in the presence of pyruvate). As expected, E2plip acted as a poor substrate for E1o with the overall extent of reductive succinylation being only 11% of the value achieved by wt E2olip (Figure 3a). The overall extent of reductive succinylation of E2olipLS within the timeframe of the experiment was also lower than wt E2olip, with the mutant domain retaining 21% less of the succinyl group after 25 min than wt E2olip (Figure 3a). The reductive succinylation

rate of E2olipLS was also lower than the wild-type E2olip, with the initial rate dropping from *ca* 368 pmole succinyl group incorporated per min for wt E2olip to 14 for E2olipLS (Figure 3b). The additional A17V-T18E mutations incorporated into E2olipLS+ further reduced the domains ability to be reductively succinylated (Figure 3). The overall extent of reductive succinylation of E2olipLS+ was only 30% of the wt E2olip value and the rate was barely detectable.

Deletion of six residues from the loop had a more dramatic effect, with E2olipLD losing its capacity to become reductively succinylated (Figure 3a). Even wt E2olip was reductively succinylated to a greater extent than E2olipLD.

Exchanging the E2olip loop for its equivalent sequence in E2olip improved the ability of the domain to productively interact with E1p, as E2olipLS was reductively acetylated to a greater extent than wt E2olip (Figure 4a). The wt E2olip was, as expected, a poor substrate for E1p as the overall extent of reductive acetylation of the domain being only 3% the value obtained for wt E2olip (Figure 4a). The overall extent of reductive acetylation of E2olipLS was *ca* 10 fold higher than that of the wt E2olip (Figure 4a). This was still 72% lower than that achieved by wt E2olip (Figure 4a) and the reductive acetylation rate of E2olipLS was very low (Figure 4b). Both the rate and overall extent of reductive acetylation of E2olipLS+ was nominal, with values similar to that of wild-type E2olip (Figure 4) suggesting that the additional mutations in β -strand 2 do not contribute to interaction with E1 and probably have a negative contribution.

Reductive acylation of the E2olip T42G and V45A variants

Mutation of the XDK residue of E2olip had a significant effect on the domain's ability to be reductively succinylated by E1o. The overall extent of reductive succinylation of the E2olipT42G variant was 43% lower than that observed for wt E2olip and 12% lower than the E2olipLS variant (Figure 3a). The reductive succinylation rate of E2olipT42G was also substantially slower than that observed for wt E2olip (Figure 3b), with the initial rate dropping to 11 pmole of succinyl group incorporated per minute, just below that observed for the E2olipLS. When the T42G mutation was combined with the loop exchange, the efficiency of reductive succinylation was reduced further. The overall extent of reductive succinylation of E2olipLS-T42G drops by 22% and 34% compared to the values obtained for the E2olipT42G and E2olipLS variants, respectively (Figure 3a). The reductive succinylation rate of E2olipLS-T42G was significantly slower than that observed for E2olipT42G and E2olipLS, with the initial rate falling to 4 pmole succinyl group incorporated per minute (Figure 3b).

Although mutation to the XDK residue reduced the efficiency by which E1o succinylated the domain, reductive acetylation by E1p in the presence of pyruvate increased significantly above that observed for wt E2olip. The overall extent of reductive acetylation of E2olipT42G was still much lower than wt E2plip, but was nearly 5 times higher than that observed for wild-type E2olip (Figure 4a). The E2plipLS-T42G variant was an even better substrate for E1p, with the overall extent of reductive acetylation nearly 12 times higher than wild-type E2olip and significantly greater than either E2olipLS or E2olipT42G (Figure 4a). The overall extent of reductive acetylation of E2olipLS-T42G was still only 35% of that achievable with wt E2plip as substrate in the time span of the experiment (Figure 4a). The reductive acetylation rate was also very slow (Figure 4b), with an observed initial rate of *ca* 2 pmole of acetyl groups incorporated per minute compared *ca* 270 for wt E2plip.

Introducing the V45A mutation into E2olip had little effect on the domains ability to be reductively succinylated. The overall extent of reductive succinylation was essentially the same as wt E2olip (Figure 3a). The rate of reductive succinylation of E2olipV45A was lower compared to wt E2olip indicating that the mutation had some impact on the efficiency of the interaction with E1o (Figure 3b). However, this change is not as dramatic as that observed for E2plipT42G.

Influence of the loop mutations on E2olip structure

To investigate the effects of mutating the surface loop on the conformation of E2olip, both E2olipLS and E2olipLD were analysed by 2D NMR spectroscopy. Even though the loop is shorter by 2 residues, the 2D homonuclear NOESY spectrum of the E2olipLS domain suggested that it has a similar structure to wild-type domain (Figure 5a). The crosspeaks in the H^N - H^α regions were well dispersed with many present downfield of the 1H_2O signal signifying a β -sheet structure. Most of the crosspeaks had chemical shift values close to that of wt E2olip suggesting that their structures were very similar (Figure 5b). Three regions of E2olipLS demonstrated a significant change in chemical shift; residues in the adjacent β -strand 2, residues in and flanking the lipoyl-lysine β -turn region and residues in and flanking β -strand 7. All these regions are close in space to the mutated loop in the structure of E2olip (Figure 1). The largest changes in chemical shift occurred for residues in the lipoyl-lysine region. The most notable concerned Thr42 (Figure 5b), whose H^α resonance underwent the largest change in chemical shift with a $\Delta\delta$ of 0.46 ppm. This implies that the lipoyl-lysine β -turn region, especially Thr42, is closely associated with the loop in the structure of E2olip.

The 2D homonuclear NOESY spectrum of E2olipLD was very different to that of wt E2olip suggesting that removal of six residues from the loop had a major effect on the conformation of the protein. The crosspeaks in the H^N - H^α region of E2olipLD were poorly

dispersed compared to the wild-type and the loss of crosspeaks downfield of the $^1\text{H}_2\text{O}$ signal suggests a significant disruption to the native β -sheet structure (Figure 6a and b). There was some evidence to suggest that the E2olipLD was not fully unfolded but did contain some structure. The presence of crosspeaks downfield of the $^1\text{H}_2\text{O}$ signal suggests that there was some residual β -sheet structure. Although the spectra of E2olipLD were poorly dispersed so hindering resonance assignment, some of better resolved crosspeaks were speculatively assigned (data not shown). Most of the assigned resonances lie in the lipoyl-lysine β -turn and C-terminal half of the protein. Another key indicator of E2olip structure is the resonances associated with the hydrophobic core residue Trp23, especially those with a contribution from the $\text{H}^{\epsilon 1}$ nuclei attached to the indole nitrogen. Two resonances were associated with this nucleus in E2olipLD (Figure 6c). One had a chemical shift of 10.65 ppm similar to that observed in wild-type E2olip. The second observed only for E2olipLD was at 10.1 ppm, which was closer to the random coil chemical shift for this particular proton (10.2 ppm). This suggests that the side chain of this particular residue is in slow two-state conformational exchange on the time scale of the NMR experiment. The two strong crosspeaks associated with Trp23 $\text{H}^{\epsilon 1}$ at *ca* 7.2 and 7.6 ppm observed for all species (Figure 6c) corresponds to intra-residue NOEs to the $\text{H}^{\delta 1}$ and $\text{H}^{\zeta 2}$ protons, respectively. The two weak crosspeaks at *ca* 8.4 and 9.8 observed only in the NOESY spectrum of wild-type E2olip (Figure 6c) correspond to inter-residue NOEs to Asp63 H^{N} and Glu64 H^{N} protons, respectively. The absence of these crosspeaks from the NOESY spectrum of E2olipLD, especially with relation to the $\text{H}^{\epsilon 1}$ resonance at 10.65 ppm, could be attributed to exchange broadening. Several inter-residue NOE crosspeaks associated with Trp23 $\text{H}^{\epsilon 1}$ were observed in the NOESY spectrum of both wt E2olip and E2olipLD, providing evidence that in at least one state of E2olipLD has some native-like structure (Supplementary Figure 1). However, these crosspeaks were substantially weaker in the NOESY spectrum of E2olipLD, with the low intensity crosspeaks in the wt E2olip spectrum missing from the E2olipLD spectrum.

Influence of T42G mutation on E2olip structure

Considering the influence of the T42G mutation on both lipoylation and reductive acylation, the relationship of Thr42 with the prominent surface loop and the rest of E2olip was investigated by NMR. The 2D ^{15}N HSQC spectra of E2olipT42G and the wild-type domain were compared. Generally, the spectrum of E2olipT42G was well dispersed and characteristic of β -sheet-containing protein, being very similar to that of wt E2olip domain. While most of the resonances derived from residues associated with E2olipT42G had similar chemical shift values to their counterparts in wt E2olip, suggesting that they share a common overall structure, several diverged significantly (Figure 7). The residues

immediately to the C-terminal of Thr42 underwent the largest change in chemical shift, followed by residues in the surface loop. In fact, after Asp43 and Lys44, Ser14 and Val15 in the loop underwent the largest change in chemical shift, slightly greater than that observed for Glu41 that is immediately to the N-terminal of the mutated residue (Figure 7). Residues Thr67 to Gln72 in β -strand 7 and in the turn connecting β -strand 7 to 8 also undergo a smaller yet significant change in chemical shift. This region and Thr42 are not in direct contact but are separated by the surface loop (Figure 1a).

Discussion

Specific post-translational modification and reductive acylation are essential properties of the lipoyl domains from 2-oxo acid dehydrogenase complexes. Lipoylation of the correct lysine residue and subsequent reductive acylation of the lipoyl group by the cognate E1 component are both governed by precise protein-protein interactions between the lipoyl domain and the relevant enzyme. Evidence from analysis of lipoyl domains from PDH complexes highlights that without a structured lipoyl domain neither event will occur, or will do so at a much reduced rate [20, 29].

Lipoylation by LplA is less specific than reductive acylation as the enzyme from *E. coli* will modify lipoyl domains found in other species [18, 30, 38-40]. Lipoyl domains must have common features for this to occur, one of which the correct positioning of the lipoyl-lysine in the exposed β -turn [30]. The surface loop has been suggested as another. Replacement of loop residues in *E. coli* E2plip with the equivalent residues found in E2olip resulted in an improved rate of lipoylation [20] suggesting a role for the loop in the lipoylation process by LplA. Here we show that both wt E2olip and E2plip were lipoylated at the similar rates and that mutations to the loop residues in E2olip did not have a significant effect on lipoylation (Figure 2 and Table 1). Therefore, the original observation of increased lipoylation rate for E2plip loop mutant must therefore be due to a structural change particular to that variant, as suggested by the authors. Mutation of the XDK in E2olip (T42G) did cause a slight increase in lipoylation rate (Table 1). This is in contrast to the equivalent mutation in E2plip (G39T) that had no effect on lipoylation efficiency [20]. Therefore, in the context of E2olip, mutation of the XDK residue rather than the surface loop enhances lipoylation efficiency. Given that the surface loop and the XDK residue are closely associated in the structure of lipoyl domains, mutations in the surface loop could influence the lipoyl-lysine region and *vice versa*. This is discussed further below.

Removal of the six residues from the surface loop so as to mimic the equivalent region in the C-terminal symmetrical half of the protein had a major impact on the structure of the domain. Loop shortening was accompanied by a major change in the conformation of the protein, with the NMR data suggesting that the domain was, at best, partially folded (Figure 6). This change in structure is the likely reason for the reduced rate of lipoylation (Figure 2) and the loss of E2olipLD's reductive succinylation capacity (Figure 3). Even though NMR spectra indicated that the domain was partially folded (Figure 6 and Supplementary Figure 1), the fact that E2olipLD could be lipoylated suggests that the domain still contains features of the lipoyl domain fold. The β -turn housing the lipoyl domain has to be formed in order to present the target lysine to LplA. Therefore, this structural feature must be formed, at least

for a portion of the time, in E2olipLD for lipoylation to occur. The presence of crosspeaks downfield of the $^1\text{H}_2\text{O}$ signal suggests the protein retains some β -sheet structure (Figure 6). Two separate resonances were associated with Trp23 H^ϵ from E2olipLD, with one present at a similar chemical shift to that of wt E2olip and the other closer to the random coil value (Figure 6). The presence of two peaks suggests that this residue occupies two distinct conformational states, one equivalent to its position within the structure of wt E2olip and another, in a predominantly unstructured region. While some long-range inter-residue crosspeaks were observed for both the wt E2olip and E2olipLD H^ϵ resonance at 10.65 ppm, many were absent from the NOESY spectrum of E2olipLD (Figure 6c and Supplementary Figure 1). Their absence from the E2olipLD spectrum is most likely attributable to exchange broadening rather than loss of structure as even the observed crosspeaks were substantially weaker than their counterparts observed in the NOESY spectrum of wt E2olipLD (Supplementary Figure 1).

The characteristics of E2olipLD mirrors that for the equivalent loop deletion variant of *E. coli* E2plip [20], whereby the mutant domain also had a non-native structure but could be lipoylated albeit at a reduced rate. Recent studies have revealed that the E2plip loop deletion variant forms a dimer via a unique domain swap mechanism (Katherine Stott, University of Cambridge, personal communication) and E2olipLD could be forming or be in exchange with a similar structure. Thus lipoyl domains do not have to be correctly folded in order for lipoylation to occur providing certain structural features, such as the formation of the β -hairpin, are preserved but, a correctly folded domain acts as a better substrate for LplA. However, a folded domain is a prerequisite for a productive interaction with E1. The extra residues found in the N-terminal half of the protein obviously plays an important role in maintaining the β -barrel fold found in all lipoyl domains.

Reductive acylation of a lipoyl domain by its cognate E1 is far more demanding than lipoylation by LplA. The *E. coli* E2olip domain is recognised only by E1o (Figures 3 and 4). The specificity of the protein-protein interactions between the lipoyl domain and E1 is essential for the precise substrate channelling that occurs within PDH and 2OGDH complexes [4, 21, 22]. As E2olip and E2plip share a common fold, subtle differences in sequence and therefore structure must be responsible for instilling specificity. The prominent surface loop linking β -strands 1 and 2 (Figure 1) has been implicated for the PDH complex from *E. coli* [20, 28] and *B. stearrowthermophilus* [29, 41]. Our work here suggests that the surface loop also plays a key role in specifying the interaction between E1o and E2olip in the *E. coli* 2OGDH complex. By exchanging the loop in E2olip for the equivalent residues found in E2plip, the domain's ability to act as a substrate for the cognate E2o was substantially

reduced (Figure 3). The NMR data suggests that E2olipLS has a native-like fold (Figure 5), despite the fact that the surface loop of E2olipLS is two residues shorter than that found in wild-type E2olip (Figure 1c).

The role of the surface loop as an important element in specifying the interaction of the E2olip with E1 is further strengthened by the improved ability of E2olipLS to be reductively acetylated by E1p. The overall extent of reductive acetylation of E2olipLS was *ca* 10 fold higher than that achieved by wild-type E2olip (Figure 4). This was still below that achievable by wt E2plip, and the rate of reductive acetylation of E2olipLS was still very low (Figure 4). Therefore, decreasing the size and altering the nature of the prominent surface loop in E2olip reduced the specificity and increased the promiscuity of the domain, allowing a productive interaction with either E1o or E1p. Data present here and elsewhere [18, 20, 30] agree that the loop is a common determinant in specifying the interaction of the lipoyl domain with E1.

Unlike E2olipLS, the decreased reductive succinylation capacity of E2olipLS+ was not reciprocated by an increased ability to be acetylated by E1p (Figure 4) and suggests that Ala17 and Thr18 of β -strand 2 are not involved in the recognition processes by E1. It is more likely that mutating these residues caused a structural change in the protein that impeded the interaction with both E1o and E1p, and so causing the subsequent drop in reductive acylation.

The XDK residue of *E. coli* E2olip does appear to play an important role in determining the interaction of the domain with E1. Mutation of Thr42 to a Gly, the residue found at the same position in E2plip, significantly reduced the domain's ability to be reductively succinylated (Figure 3). Both the NMR (Figure 7) and *in vitro* lipoylation data (Table 2) suggest that the domain had a native-like conformation and that major changes to the structure of the protein are unlikely to account for the reduced capability to be reductively succinylated. The observed slight increase in the reductive acetylation capacity of E2olipT42G by E1p (Figure 4a) further substantiates the role of the XDK residue in specifying the interaction of the domain with E1.

Combining both the T42G mutation with the loop exchange reduced the ability of the domain to be succinylated to below that of the individual mutations (Figure 3). This is reciprocated by an improvement of E2olipLS-T42G to be reductively acetylated by E1p over that achieved by wt E2olip, E2olipT42G and E2olipLS (Figure 4). This infers that both regions are critical to defining the interaction with E1, at least in the context of *E. coli* E2olip. Although E2olipLS-T42G appears to be the best substrate of the different variant E2olip domains investigated here, it still acts as a poor substrate for E1p compared to the wild-type E2plip, suggesting that these regions are important but not the sole determinants for specifying the interaction with E1.

The nature of the XDK residue is linked to the size of the adjacent prominent surface loop. Lipoyl domains with larger loops tend to have an uncharged polar residue at the XDK position (e.g. Asn in *B. stearothermophilus* E2plip [29] and Thr here in *E. coli* E2olip), while domains with shorter loops have small, non-polar residues at the equivalent position (e.g. Gly in both *E. coli* and *Haemophilus influenzae* E2plip [20]). Moreover, the structurally related biotin caboxy-carrier protein from the acetyl CoA carboxylase enzyme has no surface loop linking the first and second β -strands and has an alanine at the position equivalent to the XDK position [42-45]. Structural analysis of *E. coli* E2olip reveals that Thr42 is partially buried by residues comprising the surface loop, hence would not be considered as a residue involved in direct interaction with E1o. The surface loop of *E. coli* E2olip [9] and other lipoyl domains [8, 10-12] is poorly defined due to the lack of experimental constraints suggesting it could be inherently flexible. This was backed up by experimental findings that showed both the surface loop and, to a much greater extent, the lipoyl-lysine β -turn to be dynamic in several different lipoyl domains [13, 40] including *E. coli* E2plip [8]. The role of the polar, uncharged XDK residues in domains with the longer surface loops may be to restrain flexibility via hydrogen bonding, so maintaining the conformation of the loop and the lipoyl-lysine β -turn in order to facilitate the interaction with E1. Analysis of the structure ensemble of *E. coli* E2olip revealed that for some members of the ensemble, the side-chain hydroxyl group of Thr42 was hydrogen bonded to the backbone carbonyl oxygen of Asp17 in the surface loop. The close association of Thr42 with the surface loop is obvious from the analysis of the structure and is highlighted by NMR data (Figures 5 and 7). Therefore, Thr42 may be pivotal in providing the surface loop with the required anchor to restrict conformational freedom in this region. However, it cannot be ignored that mutating Thr42 to Gly may have perturbed the structure of the lipoyl-lysine β -turn and the surface loop, so influencing the interaction of E2olip with E1.

Although the V45A mutant of E2olip did result in a slightly reduced rate of reductive succinylation compared to the wild-type, it was still substantially higher than the other variants and achieved the same level of incorporation of succinyl group as the wild-type (Figure 3). Therefore, Val45 is unlikely to play a major role in specifying the interaction with E1 even though the lipoyl-lysine DKA and DKV motifs are generally conserved in E2plip and E2olip domains, respectively.

We have shown here that the prominent surface loop linking β -strands 1 and 2 plays an important role in specifying the interaction of the lipoyl domain from *E. coli* 2OGDH with E1. Indeed, its role in determining the interaction with E1 and for maintaining a functional conformation appears to be common to all lipoyl domains from 2-oxo acid dehydrogenase

complexes. The interaction with E1 is very sensitive to changes in lipoyl domain structure, with minor deviations hindering the interaction (such as the E2olipLS or E2olipT42G variants) and major disruption abolishing recognition (e.g. E2olipLD). The lipoate protein ligase enzyme is not as sensitive to structural changes to the domain as E1, with even misfolded domains capable of becoming lipoylated. We have shown here that the simple exchange of elements involved in defining the lipoyl domain-E1 interaction, it is possible to alter the specificity of the domain to make it more promiscuous. What is apparent is that the precise interaction between the lipoyl domain and E1 is complex and although the surface loop and the XDK residue are likely to play significant roles in this process, either by direct interaction or by maintaining the domain in the correct conformation, they are not the sole determinants of recognition.

Acknowledgements

We thank the BBSRC for the award of research grants to DDJ and RNP and the BBSRC and The Wellcome Trust for support of the core facilities of the Cambridge Centre for Molecular Recognition. We thank Mr C. Fuller for the preparation of LplA and Dr Katherine Stott for running NMR experiments and advice on interpreting the data. We thank Dr Wayne Edwards for critically reading this paper.

References

- 1 Mattevi, A., de Kok, A., Perham, R.N. (1992) The pyruvate dehydrogenase multienzyme complex. *Current Opinions in Structural Biology*. **2**, 877-887
- 2 Perham, R. N. (1991) Domains, motifs, and linkers in 2-oxo acid dehydrogenase multienzyme complexes: a paradigm in the design of a multifunctional enzyme. *Biochemistry*. **30**, 8501-8512
- 3 Reed, L. J. and Hackert, M. L. (1990) Structure-function relationships in dihydrolipoamide acyltransferases. *J. Biol. Chem.* **265**, 8971-8974
- 4 Perham, R. N. (2000) Swinging arms and swinging domains in multifunctional enzymes: catalytic machines for multistep reactions. *Ann. Rev Biochem.* **69**, 961-1004
- 5 Mattevi, A., Obmolova, G., Schulze, E., Kalk, K. H., Westphal, A. H., de Kok, A. and Hol, W. G. J. (1992) Atomic structure of the cubic core of the pyruvate dehydrogenase multienzyme complex. *Science*. **255**, 1544-1550
- 6 Milne, J. L., Shi, D., Rosenthal, P. B., Sunshine, J. S., Domingo, G. J., Wu, X., Brooks, B. R., Perham, R. N., Henderson, R. and Subramaniam, S. (2002) Molecular architecture and mechanism of an icosahedral pyruvate dehydrogenase complex: a multifunctional catalytic machine. *EMBO Journal*. **21**, 5587-5598
- 7 Green, J. D. F., Laue, E.D., Perham, R.N., Ali, S.T., Guest, J.R. (1995) Three dimensional structure of a lipoyl domain from the dihydrolipoyl acetyltransferase component of the pyruvate dehydrogenase multienzyme complex of *Escherichia coli*. *J. Mol. Biol.* **248**, 328-343
- 8 Jones, D. D., Stott, K. M., Howard, M. J. and Perham, R. N. (2000) Restricted motion of the lipoyl-lysine swinging arm in the pyruvate dehydrogenase complex of *Escherichia coli*. *Biochemistry*. **39**, 8448-8459.
- 9 Ricaud, P. M., Howard, M. J., Roberts, E. L., Broadhurst, R. W. and Perham, R. N. (1996) 3D structure of the lipoyl domain from the dihydrolipoyl succinyltransferase component of the 2-oxoglutarate dehydrogenase multienzyme complex of *Escherichia coli*. *J. Mol. Biol.* **264**, 179-190
- 10 Berg, A., Vervoort, J. and deKok, A. (1997) Three-dimensional structure in solution of the N-terminal lipoyl domain of the pyruvate dehydrogenase complex from *Azotobacter vinelandii*. *Euro. J. Biochem.* **244**, 352-360
- 11 Berg, A., Vervoort, J. and de Kok, A. (1996) Solution structure of the lipoyl domain of the 2-oxoglutarate dehydrogenase complex from *Azotobacter vinelandii*. *J. Mol. Biol.* **261**, 432-442
- 12 Howard, M. J., Fuller, C., Broadhurst, R. W., Perham, R. N., Tang, J. G., Quinn, J., Diamond, A. G. and Yeaman, S. J. (1998) Three-dimensional structure of the major autoantigen in primary biliary cirrhosis. *Gastroenterology*. **115**, 139-146
- 13 Chang, C. F., Chou, H. T., Chuang, J. L., Chuang, D. T. and Huang, T. H. (2002) Solution structure and dynamics of the lipoic acid-bearing domain of human mitochondrial branched-chain alpha-keto acid dehydrogenase complex. *J. Biol. Chem.* **277**, 15865-15873
- 14 Green, D. E., Morris, T. W., Green, J., Cronan, J. E. and Guest, J. R. (1995) Purification and properties of the lipoate protein ligase of *Escherichia coli*. *Biochem. J.* **309**, 853-862
- 15 Morris, T. W., Reed, K. E. and Cronan, J. E., Jr. (1995) Lipoic acid metabolism in *Escherichia coli*: the *lplA* and *lipB* genes define redundant pathways for ligation of lipoyl groups to apoprotein. *J Bacteriol.* **177**, 1-10
- 16 Graham, L. D., Packman, L.C., Perham, R.N. (1989) Kinetics and specificity of reductive acylation of lipoyl domains from 2-oxo acid dehydrogenase complexes. *Biochemistry*. **28**, 1574-1581
- 17 Reed, L. J., Leach, F. R. and Koike, M. (1958) Studies on a lipoic acid-activating system. *J. Biol. Chem.* **232**, 123-142

- 18 Berg, A., Westphal, A. H., Bosma, H. J. and de Kok, A. (1998) Kinetics and specificity of reductive acylation of wild-type and mutated lipoyl domains of 2-oxo-acid dehydrogenase complexes from *Azotobacter vinelandii*. *Euro. J. Biochem.* **252**, 45-50
- 19 Graham, L. D. and Perham, R. N. (1990) Interactions of lipoyl domains with the Elp subunit of the pyruvate dehydrogenase multienzyme complex from *Escherichia coli*. *FEBS Lett.* **262**, 241-244
- 20 Jones, D. D., Horne, H. J., Reche, P. A. and Perham, R. N. (2000) Structural determinants of post-translational modification and catalytic specificity for the lipoyl domains of the pyruvate dehydrogenase multienzyme complex of *Escherichia coli*. *J. Mol. Biol.* **295**, 289-306
- 21 Berg, A. and de Kok, A. (1997) 2-oxo acid dehydrogenase multienzyme complexes. The central role of the lipoyl domain. *Biological Chemistry.* **378**, 617-634
- 22 Perham, R. N., Jones, D. D., Chauhan, H. J. and Howard, M. J. (2002) Substrate channelling in 2-oxo acid dehydrogenase multienzyme complexes. *Biochem. Soc. Trans.* **30**, 47-51
- 23 Arjunan, P., Nemeria, N., Brunskill, A., Chandrasekhar, K., Sax, M., Yan, Y., Jordan, F., Guest, J. R. and Furey, W. (2002) Structure of the pyruvate dehydrogenase multienzyme complex E1 component from *Escherichia coli* at 1.85 Å resolution. *Biochemistry.* **41**, 5213-5221
- 24 Ciszak, E. M., Korotchikina, L. G., Dominiak, P. M., Sidhu, S. and Patel, M. S. (2003) Structural basis for flip-flop action of thiamin pyrophosphate-dependent enzymes revealed by human pyruvate dehydrogenase. *J. Biol. Chem.* **278**, 21240-21246
- 25 Frank, R. A., Titman, C. M., Pratap, J. V., Luisi, B. F. and Perham, R. N. (2004) A molecular switch and proton wire synchronize the active sites in thiamine enzymes. *Science.* **306**, 872-876
- 26 Frank, R. A., Price, A. J., Northrop, F. D., Perham, R. N. and Luisi, B. F. (2007) Crystal structure of the E1 component of the *Escherichia coli* 2-oxoglutarate dehydrogenase multienzyme complex. *J. Mol. Biol.* **368**, 639-651
- 27 Aevarsson, A., Seger, K., Turley, S., Sokatch, J. R. and Hol, W. G. (1999) Crystal structure of 2-oxoisovalerate dehydrogenase and the architecture of 2-oxo acid dehydrogenase multienzyme complexes. *Nat. Struct. Biol.* **6**, 785-792.
- 28 Jones, D. D., Stott, K. M., Reche, P. A. and Perham, R. N. (2001) Recognition of the lipoyl domain is the ultimate determinant of substrate channelling in the pyruvate dehydrogenase multienzyme complex. *J Mol. Biol.* **305**, 49-60.
- 29 Wallis, N. G., Allen, M.D., Broadhurst, R.W., Lessard, I.A.D., Perham, R.N. (1996) Recognition of a surface loop of the lipoyl domain underlies substrate channelling in the pyruvate dehydrogenase multienzyme complex. *J. Mol. Biol.* **263**, 436-474
- 30 Wallis, N. G. and Perham, R. N. (1994) Structural dependence of post-translational modification and reductive acetylation of the lipoyl domain of the pyruvate dehydrogenase multienzyme complex. *J. Mol. Biol.* **236**, 209-216
- 31 Reche, P., Li, Y. L., Fuller, C., Eichhorn, K. and Perham, R. N. (1998) Selectivity of post-translational modification in biotinylated proteins: the carboxy carrier protein of the acetyl-CoA carboxylase of *Escherichia coli*. *Biochem J.* **329**, 589-596
- 32 Ho, S. N., Hunt, H. D., Horton, R. M., Pullen, J. K. and Pease, L. R. (1989) Site-directed mutagenesis by overlap extension using the polymerase chain reaction. *Gene.* **77**, 51-59
- 33 Horton, R. M., Hunt, H. D., Ho, S. N., Pullen, J. K. and Pease, L. R. (1989) Engineering hybrid genes without the use of restriction enzymes - gene-splicing by overlap extension. *Gene.* **77**, 61-68
- 34 Dardel, F., Packman, L. C. and Perham, R. N. (1990) Expression in *Escherichia coli* of a sub-gene encoding the lipoyl domain of the pyruvate dehydrogenase complex of *Bacillus stearothermophilus*. *FEBS Lett.* **264**, 206-210

- 35 Jeener, J., Meier, J., Bachmann, P. and Ernst, R. R. (1979) Investigation of the exchange processes by two-dimensional NMR spectroscopy. *J. Chem. Phys.* **71**, 323-341
- 36 Kumar, A., Ernst, R.R. & Wuthrich, K. (1980) A two-dimensional nuclear Overhauser enhancement experiment for the elucidation of complete proton-proton cross-relaxation networks in biological macromolecules. *Biochem. Biophys. Res. Commun.* **95**, 1-6
- 37 Kraulis, P. J. (1989) ANSIG - a program for the assignment of protein H-1 2D NMR spectra by interactive computer graphics. *J. Mag. Res.* **84**, 627-633
- 38 Macherel, D., Bourguignon, J., Forest, E., Faure, M., Cohen Addad, C. and Douce, R. (1996) Expression, lipoylation and structure determination of recombinant pea H-protein in *Escherichia coli*. *Euro. J. Biochem.* **236**, 27-33
- 39 Quinn, J., Diamond, A. G., Masters, A. K., Brookfield, D. E., Wallis, N. G. and Yeaman, S. J. (1993) Expression and lipoylation in *Escherichia coli* of the inner lipoyl domain of the E2-component of the human pyruvate dehydrogenase complex. *Biochem. J.* **289**, 81-85
- 40 Tozawa, K., Broadhurst, R. W., Raine, A. R., Fuller, C., Alvarez, A., Guillen, G., Padron, G. and Perham, R. N. (2001) Solution structure of the lipoyl domain of the chimeric dihydrolipoyl dehydrogenase P64K from *Neisseria meningitidis*. *Eur. J. Biochem.* **268**, 4908-4917
- 41 Howard, M. J., Chauhan, H. J., Domingo, G. J., Fuller, C. and Perham, R. N. (2000) Protein-protein interaction revealed by NMR T(2) relaxation experiments: the lipoyl domain and E1 component of the pyruvate dehydrogenase multienzyme complex of *Bacillus stearothermophilus*. *J Mol Biol.* **295**, 1023-1037
- 42 Athappilly, F. K. and Hendrickson, W. A. (1995) Structure of the biotinyl domain of acetyl-coenzyme A carboxylase determined by MAD phasing. *Structure.* **3**, 1407-1419
- 43 Roberts, E. L., Shu, N., Howard, M. J., Broadhurst, R. W., Chapman-Smith, A., Wallace, J. C., Morris, T., Cronan, J. E., Jr. and Perham, R. N. (1999) Solution structures of apo and holo biotinyl domains from acetyl coenzyme A carboxylase of *Escherichia coli* determined by triple-resonance nuclear magnetic resonance spectroscopy. *Biochemistry.* **38**, 5045-5053
- 44 Reddy, D. V., Shenoy, B. C., Carey, P. R. and Sonnichsen, F. D. (2000) High resolution solution structure of the 1.3S subunit of transcarboxylase from *Propionibacterium shermanii*. *Biochemistry.* **39**, 2509-2516
- 45 Yao, X., Wei, D., Soden, C., Jr., Summers, M. F. and Beckett, D. (1997) Structure of the carboxy-terminal fragment of the apo-biotin carboxyl carrier subunit of *Escherichia coli* acetyl-CoA carboxylase. *Biochemistry.* **36**, 15089-15100

Figure 1. (a) The structure of *E. coli* E2olip ([9]; PDB: 1pmr). The lipoyl-lysine β -turn is coloured red, with the lipoyl-lysine highlighted as ball-and-stick and residues Thr42 and Val45 shown as spheres. The prominent surface loop is coloured orange. The positions and numbering of β -strands are shown on the structure. (b) Sequence alignment of the quasi-symmetrical N- and C-terminal halves of E2olip. Residues that are identical and highly conserved between the two halves of the domain are shown in bold. Residues are coloured as in (a). (c) Description of the wild-type and mutant *E. coli* lipoyl domains constructed and analysed in this study.

Figure 2. *In vitro* lipoylation of wt E2plip, wt E2olip and E2olipLD by *E. coli* LplA. In each lane, the upper band (-) represents the apo form of the domain and the lower band (+) represents the lipoylated domain. The presence of doublet bands present for the wt E2plip samples was probably due to partial processing of the N-terminal methionine residue, as reported previously [20], although deamidation of an asparagine or glutamine residue cannot be ruled out.

Figure 3. Reductive succinylation of the lipoyl domains by E1o in the presence of 2-oxoglutarate. (a) The overall extent of reductive succinylation of the lipoyl domains by E1o after 25 min. The activity refers to the percentage of succinyl group incorporated compared to wt E2olip. The average value for wt E2olip was $0.63 \text{ nmol} \pm 0.04$ of [^{14}C] succinyl group incorporated per nmol of lipoyl domain, similar to previous observations [20]. (b) The rate of reductive succinylation of the wt E2olip (\circ), E2olipLS (\blacksquare), E2olipLS+ (\square), E2olipT42G (\blacklozenge), E2olipLS-T42G (\diamond), E2olipV45A (\times) and wt E2plip (\bullet) by E1o.

Figure 4. Reductive acetylation of the lipoyl domains by E1p in the presence of pyruvate. (a) The overall extent of reductive acetylation of the lipoyl domains by E1p after 25 min. Activity refers to the percentage of acetyl group incorporated compared to wt E2plip. The average value for wt E2plip was $0.70 \text{ nmol} \pm 0.06 \text{ nmol}$ of [^{14}C] acetyl group incorporated per nmol of lipoyl domain, similar to previous observation [20]. (b) The rate of reductive acetylation of wt E2plip (\bullet), E2olipLS (\blacksquare), E2olipT42G (\blacklozenge), E2olipLS-T42G (\diamond) and E2olip (\circ) by E1p.

Figure 5. NMR analysis of E2olipLS. (a) Fingerprint $\text{H}^\alpha\text{-H}^\text{N}$ region from the 2D NOESY spectrum of E2olipLS. (b) Chemical shift differences of H^α (\blacksquare) and H^N (\square) between wt

E2olip and E2olipLS. The differences were obtained by subtracting the chemical shifts of wt E2olip from those of E2olipLS. The secondary structure of E2olip is shown above the graph.

Figure 6. Fingerprint H^{α} - H^N region from 2D homonuclear NOSEY spectra of the (a) wt E2olip and (b) E2olipLD. (c) Spectra slices representing crosspeaks associated with $H^{\epsilon 1}$ of Trp23 from wt E2olip and E2olipLD. NOE connectivities associated with each crosspeak are specified on the diagram.

Figure 7. Chemical shift changes in $^1H^N$ (■) and ^{15}N (□) chemical shifts between wt E2olip and E2olipT42G. The chemical shift differences were calculated based on assignments from 2D ^{15}N HSQC spectra. The chemical shift differences relating to ^{15}N were normalised to 1H values as described in the materials and methods so that the magnitude of change for both nuclei is comparable.

Table 1. Analysis of post-translational modification of the lipoyl domains by positive-ion electrospray mass spectrometry

| Lipoyl domain | Mass of unlipoylated component (Da) | | Mass of lipoylated component (Da) | | Full lipoylation observed (min) |
|---------------|-------------------------------------|-------------------|-----------------------------------|-------------------|---------------------------------|
| | Calculated | Measured | Calculated | Measured | |
| E2olip wt | 9727 | 9727.4±0.8 | 9915 | 9915.6±1.0 | 60 |
| E2olipLS | 9487 | 9487.8±0.4 | 9676 | 9674.9±0.6 | 60 |
| E2olipLS+ | 9543 | 9542.9±0.5 | 9732 | 9731.4±0.5 | 60 |
| E2olipLD | 9128 | 9127.8±0.4 | 9316 | 9316.3±0.2 | >60 |
| E2olipT42G | 9683 | 9682.4±0.3 | 9872 | 9871.6±0.7 | 45 |
| E2olipLS-T42G | 9443 | 9442.5±1.0 | 9632 | 9631.5±0.8 | 45 |
| E2plip wt | 9108 (-Met) | 9107.0±0.4 (-Met) | 9296 (-Met) | 9297.1±0.6 (-Met) | Not determined |
| | 9239 (+Met) | 9238.5±1.1 (+Met) | 9427 (+Met) | 9425.7±1.0 (+Met) | |

Figure 1

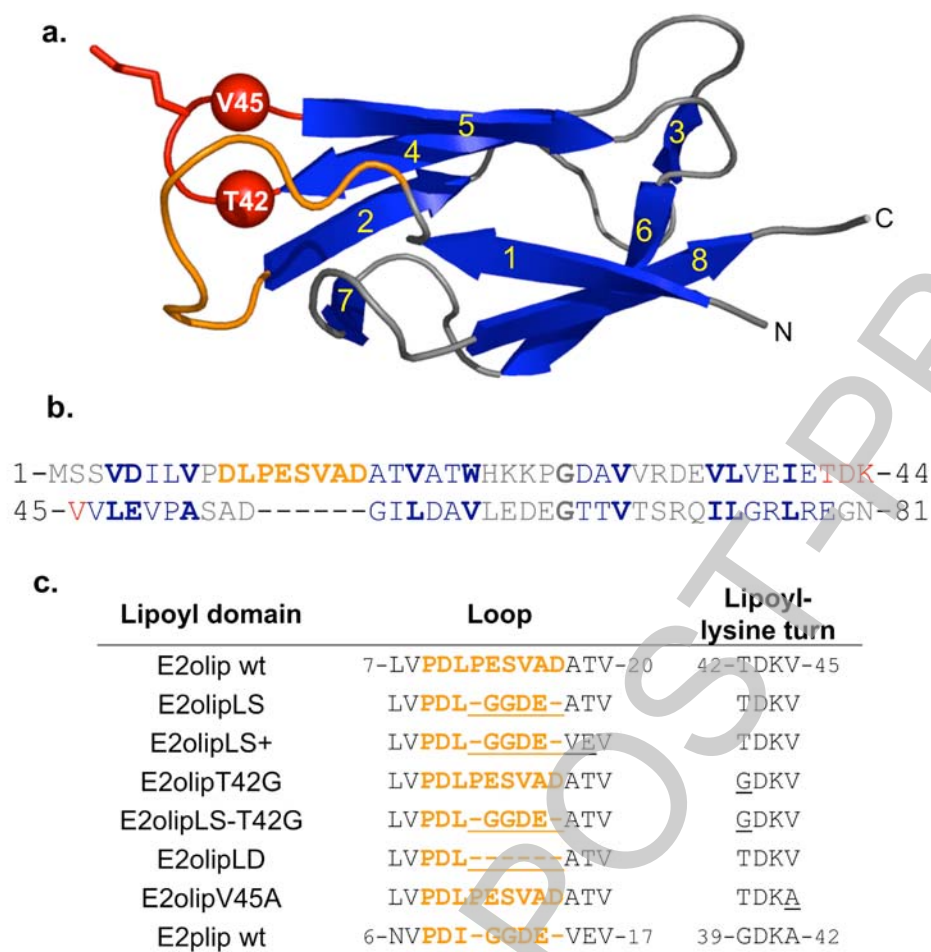


Figure 2

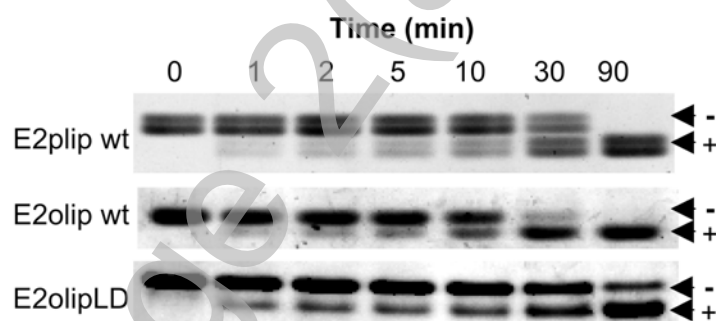


Figure 3

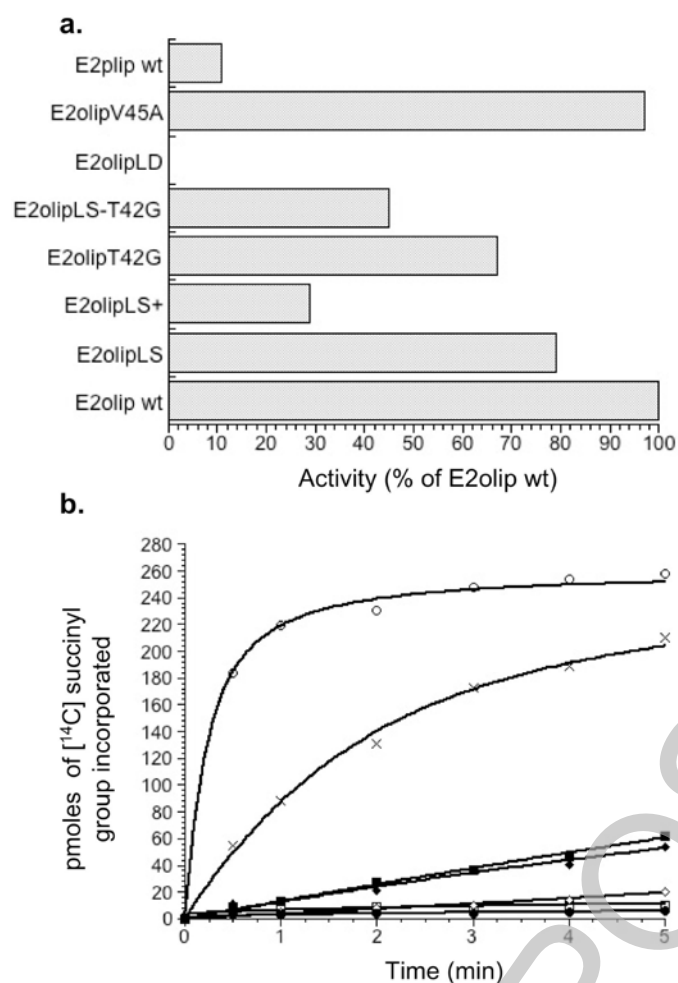


Figure 4

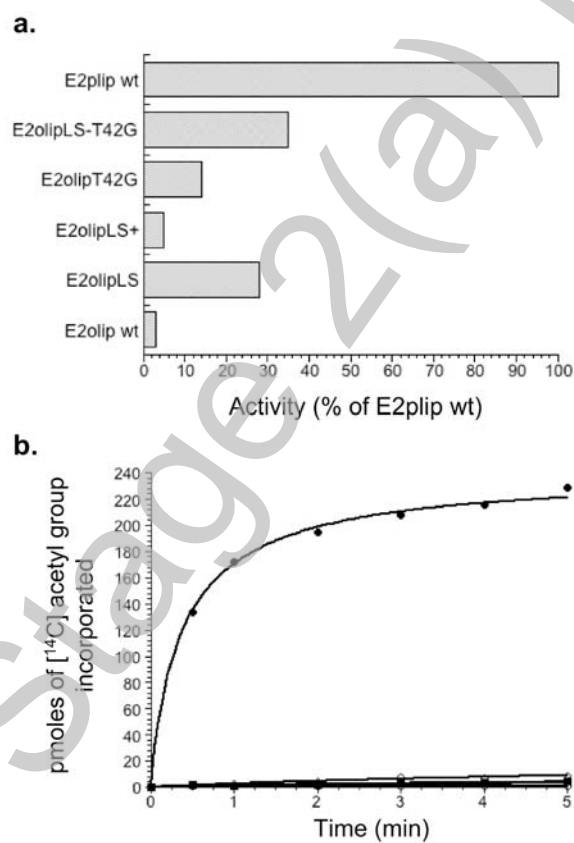


Figure 5

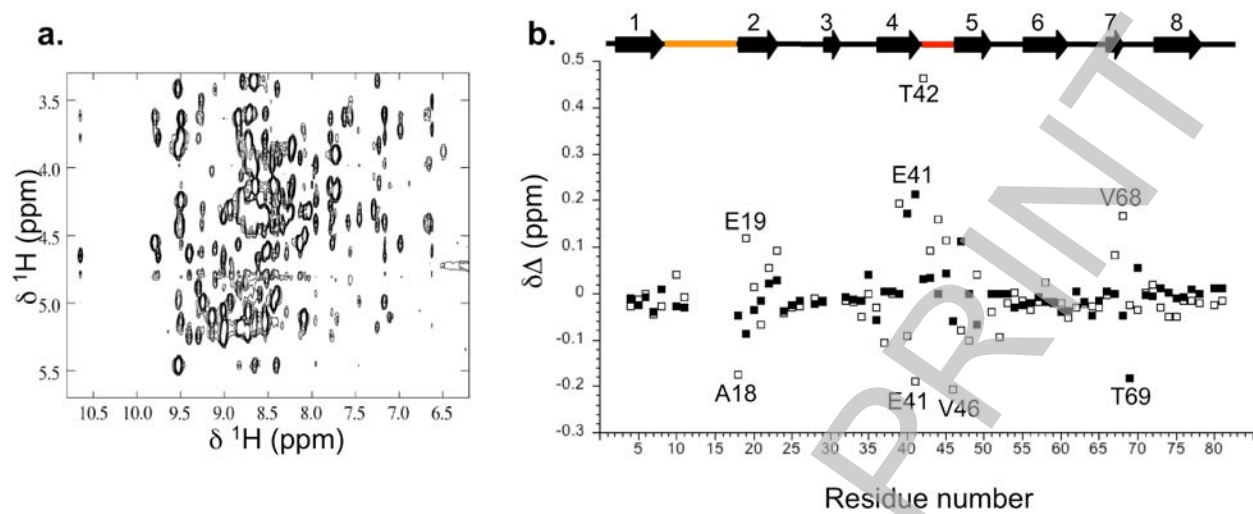


Figure 6

